Thermochimica Acta 654 (2017) 191–202

Contents lists available at ScienceDirect

Thermochimica Acta

journal homepage: www.elsevier.com/locate/tca

Thermal degradation kinetics of plastics and model selection

Pallab Das, Pankaj Tiwari*

Department of Chemical Engineering, Indian Institute of Technology Guwahati, Guwahati, Assam, 781039, India

ARTICLE INFO

Keywords:
Plastics
Thermal degradation kinetics
Isoconversional methods
Kinetic model selection

ABSTRACT

The thermal decomposition behaviour of high and low-density polyethylene (LDPE and HDPE), polypropylene (PP), poly(lactic acid) (PLA) were investigated under inert condition by dynamic thermogravimetric analysis (TGA) in the temperature range of 303–973 K at seven different heating rates. Determination of distributed activation energy at various stages of degradation process and their implication in degradation process was investigated with the help of isoconversional methods. Reaction models ($f(\alpha)$) were predicted using Criados masterplots. Corresponding values of pre-exponential factors were calculated using compensation effect. A comparative study of various isoconversional methods/models like Friedman, Kissinger-Akahira-Sunnose, Ozawa- Flynn and Wall (OFW), Starink and advance isoconversional method (AIC) was discussed and reliability of all these methods was examined. Reconstruction of the conversion profiles for different thermal history was performed and compared with experimental data to select the appropriate model.

1. Introduction

Waste plastic is one of the major contributors to the municipal solid waste. India generates 5.6 million tons of plastic waste annually [1]. Most of the commercial plastics are non-biodegradable and responsible for various environmental and ecological problems. With the increase of human population and development activities, the plastic consumption is also increasing at a higher rate. Landfilling and incineration, two most commonly used waste disposal techniques are not sustainable enough because of the lack of available land for dumping and harmful emissions respectively. Pyrolysis of waste plastic can transform solid waste into a wide range of valuable chemicals and hydrocarbon compounds [2]. Designing and implementation of the pyrolysis process for complex materials like plastics depends primarily on kinetic analysis. The precision of the pyrolysis kinetics heavily depends upon the reliable evaluation of the kinetic triplets, activation energy (E_α), pre-exponential factor (A_α) and reaction model ($f(\alpha)$). Degradation of plastics includes all changes related to chemical structure and physical properties due to external stresses. The mechanism of thermal degradation of plastics is complex in nature. Thermal degradation involves the occurrence of molecular scission which leads to the changes in molecular weight distribution of the material. This phenomenon is decisive for recycled plastics because they suffer a continuous change in temperature [3,4]. Heating any organic or inorganic solid results in many physico-chemical phenomena like melting, sublimation, polymorphic transformation, desolvation or degradation, etc [5]. TGA provides the pathway to determine the macroscopic kinetics of these processes. The microscopic kinetic accounts for simultaneously occurring multistep phenomena and requires computational methods. Isoconversional methods recommended by the International Confederation for Thermal Analysis Calorimetry (ICTAC) are able to capture the complexity involved in the process of thermal degradation of solid [6–11]. Isoconversional methods use the thermal degradation data at different temperature program and calculate the distribution of activation energy as reaction/process progresses [12]. The variable activation energy explains the complexity of the thermal degradation process at various stages of conversion process. In general single activation energy is comprehensively corresponding to gas phase reactions, whereas any condensed phase or solid phase reactions the activation energy becomes a function of temperature dependent properties of reaction media such as progress of reaction. Variable activation energy gives more mechanistic approach of complex reactions link to the energy barrier of individual steps, diffusion through solid matrix and secondary reactions etc [13].

The aim of the current study is to compare the quantitative aspects of the thermal decomposition process for four different plastics low density polyethylene (LDPE), high density polyethylene (HDPE), polypropylene (PP) and polylactic acid (PLA), which are mainly used for packaging purpose. Five different isoconversional models, namely Friedman (FR) [13], Ozawa Flynn and Wall (OFW) [14,15], Kissinger Akahira and Sunnose [16], Starink [17] and advance isoconversional models (AIC) [18] are considered. The broader aspects of the study are to understand the complex degradation reaction mechanism under pyrolysis condition and the applicability of the various isoconversional

* Corresponding author.
E-mail addresses: pankaj.tiwari@iitg.ernet.in, tpankaj81@gmail.com (P. Tiwari).

http://dx.doi.org/10.1016/j.tca.2017.06.001
Received 31 March 2017; Received in revised form 31 May 2017; Accepted 3 June 2017

Nomenclature

a	$1/RT_\alpha$
A	Pre-exponential factor (min^{-1})
A_α	Distributed pre-exponential factor with conversion (min^{-1})
AIC	Advance isoconversional method
b	$ln((d\alpha/dt)_\alpha)$
DSC	Differential scanning calorimetry
DTG	Differential thermal gravimetric
E	Activation energy *(kJ/mol)*
E_α	Distributed activation energy with conversion (kJ/mol)
$f(\alpha)$	Reaction mechanism
$g(\alpha)$	Integral form of rate equation
HDPE	High density polyethylene
i	Various temperature program (ranging from *1– n, n* being the total number of temperature program)
j	Suffix represents the temperature program other than i^{th} program, $i \neq j$
J	Symbol represents integral function
IKP	Invariant kinetic parameter
KAS	Kissinger-Akahira-Sunnose
LDPE	Low density polyethylene
OFW	Ozawa-Flynn-Wall
PE	Polyethylene
PLA	Polylactic acid
PP	Polypropylene
R	Universal gas constant (8.314 $Jmol^{-1} K^{-1}$)
T	Temperature (K)
T_α	Distributed temperature with conversion (K)
T_o	Onset degradation temperature (K)
T_e	End degradation temperature (K)
T_m	Peak temperature (K)
t	Time (min)
t_α	Time corresponding any particular conversion *(α)*
TGA	Thermal gravimetric analysis
W	Weight of sample at any temperature during degradation (mg)
W_0	Initial weight of the sample (mg)
W_∞	Residual weight, *(mg)*
α	Conversion
$Z(\alpha)$	$f(\alpha) \times g(\alpha)$
Φ	Minimization function of E_α

methods and their limitations. Selection of material is totally based on their availability in plastic waste stream except PLA, which is chosen because of its growing presence in medical field and food packaging, which also have complex molecular structure due to presence of oxygen which may create complexity in the post-consumer disposal processes like pyrolysis and combustion.

Isoconversional methods were employed to evaluate the decomposition kinetics of HDPE [19], PS and PE [20], PP [21], tyre rubber [22], biomass [23,24], coal [25], cellulose [26], and polymer composites [27,28] etc. Most of the previous studies able to utilize the way of measuring distributed activation energy and their applications. However, a few studies have captured the essence of kinetic triplet (E, A and f(α), which represent the whole understanding of any reaction. The current study successfully demonstrates the variable activation energy (E_α) with the extent of the progress of the reaction for LDPE, HDPE, PP and PLA and also at the same time considers the possibility of a distributed pre-exponential factor (frequency factor) (A_α). Distributed pre-exponential factor (A_α) actually compensate a logarithmic linear relationship with the variable activation energy, which ultimately helps to reconstruct the degradation plot and can further help to verify the calculated kinetic parameters. The kinetic parameters were obtained by applying various isoconversional methods to experimental TGA data and were examined critically. The presented results and methodology will be applicable for selecting appropriate strategies for analysis of kinetic parameters from TGA, particularly for the study of degradation kinetic of plastics, biomass, coal and composites.

2. Materials and methods

2.1. Materials

LDPE, HDPE, and PP were procured from Haldia Petrochemicals Limited, India and PLA was obtained from Nature Works®. Physical properties of plastic samples like density, glass transition temperature and melting point are reported in Table 1. The material received were in pellet form of size around 3–5 mm. The collected materials were manually cut to make 1–2 mm average particle size before subjected to TGA analysis.

2.2. Methods

The thermal degradation study was carried out using TGA (NETZSCH 209 F1 TG) equipment in the inert environment (N_2 gas) with a flow rate of 60 ml/min (40 ml/min as purge and 20 ml/min as protective gas) at seven heating rates, 5, 10, 15, 20, 30, 40, 50 K/min in the temperature range of 303–973 K. The heating rates were chosen in the range of 5 K/min to 50 K/min taking consideration of both slow pyrolysis and fast pyrolysis scenario. Industrially all these heating rates are applicable, directly or indirectly. Generally, the rate of heat absorption for any material is subjected to the thermal conductivity and the available surface area of the material. Industrially, very high heating rate and uniform distribution of heat can be achieved by using fluidised bed pyrolyser. The kinetic parameters obtained with chosen heating rates captured both slow and fast pyrolysis processes and help in accurately extrapolate the profiles for both lower and higher heating rates. Constant N_2 flow rate, particle size (1–2 mm) and initial weight (6–7 mg) were maintained for all the experiments. Differential Scanning Calorimetry (DSC) [make of Metler-Toledo with temperature range −30 °C–200 °C (from ambient to −30 °C then to 200 °C and finally bring the temperature to ambient) with a program of constant heating rate of 5 °C/min] was used to determine the melting points while densities and glass transition temperatures were provided by the manufacturer (Table 1).

2.3. Processing of TGA data

The decomposition profiles at seven different heating rates obtained from the TGA are shown in Fig. 1. TGA registers the change in mass of the sample with temperature (or time) at the specified gas environment and heating rate under a certain temperature range. Weight loss data then converted into conversion, $\alpha = (W_0 - W)/(W_0 - W_\infty)$.

Table 1
Physical properties of materials.

Plastics	Density (g/cc)	Glass transition temperature (K)	Melting point (K)
LDPE	0.934	148	384 ± 2
HDPE	0.950	193	405 ± 1
PP	0.9	263	441 ± 1
PLA	1.25	330 ± 3	443 ± 1

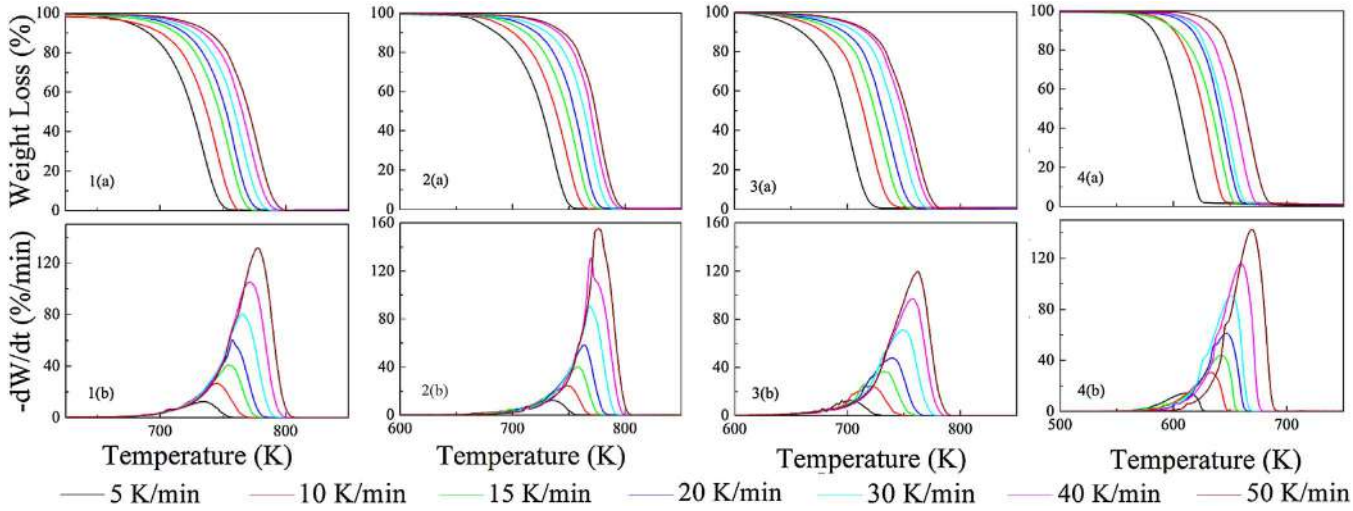

Fig. 1. Thermal degradation profile for (a) TGA, (b) DTG of (1) LDPE, (2) HDPE, (3) PP, (4) PLA at seven heating rates (5, 10, 15, 20, 30, 40, 50 K/min).

The generalized form of kinetic equation,

$$\frac{d\alpha}{dt} = k(T)f(\alpha) \tag{1}$$

Where $k(T)$ and $f(\alpha)$ are temperature dependent rate constant and mass dependent reaction model. The rate constant $k(T)$ is assumed to follow the Arrhenius law, where the temperature and time coordinates are related as $T = T_0 + \beta t$. The value of $d\alpha/dT$ are calculated numerically from temperature (T) and conversion (α) data.

$$\beta\frac{d\alpha}{dT} = A\exp\left(\frac{-E}{RT}\right)f(\alpha) \tag{2}$$

Where, $\beta = dT/dt$, represents the heating rate. Mathematical manipulation of Eq. (2) can lead to the determination of kinetic triplets (E, A and $f(\alpha)$) by fitting the degradation data obtain from TGA.

2.4. Isoconversional methods

Isoconversional method is a powerful and most reliable tool for the calculation of kinetic parameters like activation energy [17,29]. The major advantage of isoconversional method is that its eligibility to predict kinetic parameters (model free basis) without the presumption of any reaction model ($f(\alpha)$). By definition the isoconversional methods are based on the principle that, at any constant conversion the reaction rate is a function of temperature [10] so that

$$\left[\frac{\partial \ln(d\alpha/dt)}{\partial T^{-1}}\right]_{\alpha} = -\frac{E_\alpha}{R} \tag{3}$$

Various forms of isoconversional methods discussed here are based on the methodology (differential or integral) adopted to solve the rate equation (Eq. (2)). The differential form of the rate equation can be represented as

$$\ln\left(\frac{d\alpha}{dt}\right)_{\alpha,i} = \ln\left(\beta\frac{d\alpha}{dT}\right)_{\alpha,i} = \ln[A_\alpha f(\alpha)] - \frac{E_\alpha}{RT_{\alpha,i}} \tag{4}$$

The subscript i denotes for heating rates of various temperature programs. To apply the Friedman method on integral data (e.g., TGA) entails numerical differentiation of experimental α versus T plots [13]. On the other hand the integral form of rate equation for non-isothermal temperature program with constant heating rate β can be derived from the integration of Eq. (1).

$$g(\alpha) \equiv \frac{A}{\beta}\int_0^t exp\left(\frac{-E_\alpha}{RT}\right)dT = \frac{A}{\beta}I(E_\alpha, T) \tag{5}$$

Since, no analytical solutions exist for $I(E, T)$, numerical integration

Table 2
List of isoconversional models considered to study the kinetics.

		Methods	Expression	Comments
Isoconversional methods	Differential	Friedman (FR) [13]	$\ln\left(\frac{d\alpha}{dt}\right)_{\alpha,i} = \ln\left(\beta\frac{d\alpha}{dT}\right)_{\alpha,i} = \ln[A_\alpha f(\alpha)] - \frac{E_\alpha}{RT_{\alpha,i}}$	Differential isoconversional method applicable for multiple heating rate data. Very sensitive to small changes in rate data.
	Integral	Ozawa Flynn Wall (OFW) [14,15]	$\ln(\beta_i) = Const - 1.052\left(\frac{E_\alpha}{RT_\alpha}\right)$	Modified general isoconversional equation (Eq.(6)) by Doyle approximation of B = 0 and C = 1.052
		Kissinger Akahira Sunose [16]	$\ln\left(\frac{\beta_i}{T_{\alpha,i}^2}\right) = Const - \frac{E_\alpha}{RT_\alpha}$	Integral isoconversional method uses Murray and White approximation in Eq. (6) i.e. B = 2 and C = 1
		Starink [17]	$\ln\left(\frac{\beta_i}{T_{\alpha,i}^{1.92}}\right) = Const - 1.0008\left(\frac{E_\alpha}{RT_\alpha}\right)$	Starink takes the value of B = 1.92 and C = 1.0008 in Eq. (6)
		Advanced Isoconversional Model (AIC) [10,18,20]	$\Phi(E_\alpha) = \sum_{i=1}^{n}\sum_{j\neq i}^{n}\frac{J[E_\alpha, T_i(t_\alpha)]}{J[E_\alpha, T_j(t_\alpha)]} = 0$	Distributed activation energy with respect to degree of conversion is determined by minimizing the function $\Phi(E_\alpha)$

is more likely to solve the equation by applying various approximations (listed in Table 2) [10,30]. A generalized linear equation can be derived from many of such approximations

$$\ln\left(\frac{\beta_i}{T^B_{\alpha,i}}\right) = const. - C\left(\frac{E_\alpha}{RT_\alpha}\right) \quad (6)$$

Various such approximations leads to the kinetic models like Ozawa-Flynn and Wall (OFW) [14,15], Kissinger-Akahira-Sunnose [16] and Starink [17] as summarized in Table 2. The activation energy (E_α) can be derived from the slope (linear regression) of the plot of the left hand side of Eq. (6) and $1/T_\alpha$ by utilizing all the heating rate under isoconversional principle.

More accuracy of kinetic analysis can be accomplished using numerical integration. One such method is advance isoconversional method (AIC). Vyazovkin et al. [10,12,31] developed advanced isoconversional (AIC) method which utilizes numerical integration of $I(E_\alpha, T_{\alpha i}) = p(x)$Where $p(x) = \int_0^\infty e^{-x}/x^2 dx$and $x = E_\alpha/RT$.

AIC method can be applied for any arbitrary temperature programs $T_i\ (t)$ including cooling processes (negative heating rate). The value of E_α at each conversion is determined by minimizing the following function.

$$\Phi(E_\alpha) = \sum_{i=1}^{n} \sum_{j\neq i}^{n} \frac{J[E_\alpha, T_i(t_\alpha)]}{J[E_\alpha, T_j(t_\alpha)]} = 0 \quad (7)$$

Where, the temperature integral:

$$J[E_\alpha, T_i(t_\alpha)] \equiv \int_{t_{\alpha-\Delta\alpha}}^{t_\alpha} \exp\left[\frac{-E_\alpha}{RT_i(t_i)}\right] dt \quad (8)$$

has been solved numerically. Minimization was repeated for every conversion to obtain a relative dependency between E_α and α.

2.5. Reaction model

Model free isoconversional method allows evaluating the distribution of activation energy without any reaction model considered. As a part of the kinetic triplet the reaction model ($f(\alpha)$) actually determines the possible reaction mechanism of thermal degradation. AIC method provides combined pre-exponential factor and reaction model $A_\alpha \cdot f(\alpha)$ as a function of conversion using isoconversional principle. The values of pre-exponential factor can be determined by identifying reaction model using Criados masterplots [32]. The Criado method compares experimental TGA results with established frequently used reaction models as tabulated in Table 3. The method uses the following equation derived from Eq. (1) and (5).

$$\frac{z(\alpha)}{z(0.5)} = \frac{f(\alpha)g(\alpha)}{f(0.5)g(0.5)} = \left(\frac{T_\alpha}{T_{0.5}}\right)^2 \frac{(d\alpha/dt)_\alpha}{(d\alpha/dt)_{0.5}} \quad (9)$$

Where $T_{0.5}$ and $(d\alpha/dt)_{0.5}$ represent temperature and rate at α = 0.5. The purpose of dividing by 50% condition is to normalize the $z(\alpha)$

Table 3
Reaction models of most common reaction mechanism considered in solid-state reactions [10,36].

Reaction Model	Model Code	$f(\alpha)$	$g(\alpha)$
Power law	P2	$2\alpha^{1/2}$	$\alpha^{1/2}$
Power law	P3	$3\alpha^{2/4}$	$\alpha^{1/3}$
Power law	P4	$4\alpha^{3/4}$	$\alpha^{1/4}$
Avrami-Erofeev: Two-dimensional nucleation	A2	$2(1-\alpha)[-\ln(1-\alpha)]^{1/2}$	$[-\ln(1-\alpha)]^{1/2}$
Avrami-Erofeev: Three-dimensional nucleation	A3	$3(1-\alpha)[-\ln(1-\alpha)]^{2/4}$	$[-\ln(1-\alpha)]^{1/3}$
Avrami-Erofeev: Four-dimensional nucleation	A4	$4(1-\alpha)[-\ln(1-\alpha)]^{3/4}$	$[-\ln(1-\alpha)]^{1/4}$
Contracting cylinder: Two dimensional phase boundary reaction	R2	$2(1-\alpha)^{1/2}$	$1-(1-\alpha)^{1/2}$
Contracting sphere: Three dimensional phase boundary reaction	R3	$3(1-\alpha)^{2/3}$	$1-(1-\alpha)^{1/3}$
Two-dimensional diffusion	D2	$[-\ln(1-\alpha)]^{-1}$	$(1-\alpha)\ln(1-\alpha)+\alpha$
Three dimensional diffusion	D3	$3/2(1-\alpha)^{2/3}[1-(1-\alpha)^{1/3}]^{-1}$	$[1-(1-\alpha)^{1/3}]^2$
Mampel (first order)	F1	$1-\alpha$	$-\ln(1-\alpha)$
One-dimensional diffusion	D1	$1/2\alpha^{-1}$	α^2
Ginstling-Brounshtein	D4	$3/2((1-\alpha)^{-1/3}-1)$	$1-(2\alpha/3)-(1-\alpha)^{2/3}$
Second order	F2	$(1-\alpha)^2$	$(1-\alpha)^{-1}-1$
Third order	F3	$(1-\alpha)^3$	$[(1-\alpha)^{-1}-1]/2$

function. The value of $z(\alpha)/z(0.5)$ is equal to 1 at 50% conversion for most of the theoretical plots. The left hand side $[(f(\alpha)g(\alpha))/f(0.5)g(0.5)]$ is the theoretical masterplots which signifies characteristic of each reaction mechanism mentioned in Table 3. The right hand side of Eq. (9), which is also known as reduced rate was calculated from the experimental results. Comparing the theoretical masterplots with the experimental reduced rate plot suggests the most suitable reaction. For multi-heating rate data, the master plots were obtained for all the heating rates and the most suitable model has been selected by comparing the linearity coefficient (R^2) between theoretical master plots and experimental reduce plots.

Finally, the pre-exponential factor (A) can be determined by making use of Constable plot [30,33] also known as compensation method [10]. The logarithm form of rate expression can be derived from Eq. (4):

$$\ln(Af(\alpha))_\alpha = \frac{E_{a\alpha}}{RT_\alpha} + \ln\left(\left(\frac{d\alpha}{dt}\right)_\alpha\right) \quad (10)$$

In a more generalized form the equation Eq. (10) can be written as:

$$b = \ln(Af(\alpha))_\alpha - aE_\alpha \quad (11)$$

Where, $a = 1/RT_\alpha$ and $b = \ln((d\alpha/dt)_\alpha)$.

The calculated values of the activation energy (E_α) and ($A.f(\alpha)$) at various stages of conversion follows a logarithmic linear relationship and compensate each other in every stage of conversion. For a particular value α, the a and b values can be calculated. Then the values of $\ln(Af(\alpha)_\alpha)$, can be determined from the intercept of a linear plot of b and a E_α using isoconversion principle. Using the known reaction model $f(\alpha)$ predicted by Criado masterplots, the values of a preexponential factor at various extent of conversion is possible to calculate from $\ln(Af(\alpha)_\alpha)$.

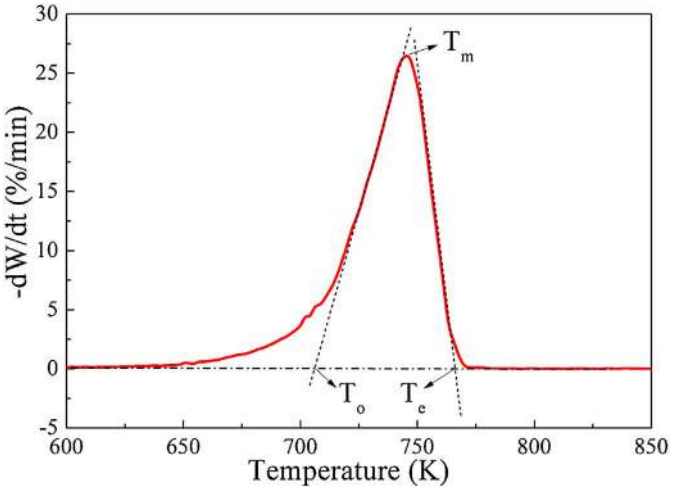

Fig. 2. Scheme adopted for the estimation of onset temperature (T_0), end temperature (T_e) and maximum degradation temperature (T_m) from DTG plot of LDPE at 10 K/min.

3. Results and discussion

3.1. TGA analysis

Thermogravimetric analysis (TGA) and derivative thermo-gravimetric (DTG) plots for LDPE, HDPE, PP and PLA at seven heating rates are shown in Fig. 1. The initial weight of the sample, heating rate, TGA temperature range, onset temperature (T_o), end temperature (T_e) and temperature at maximum degradation rate (T_m) of the degradation process are tabulated in Table 4. A scheme used for calculation of T_o, T_e and T_m from DTG curve is demonstrated in Fig. 2. Fig. 1 and Table 4

Table 4
TGA analysis: Degradation temperature range, onset, end and maximum degradation temperatures.

Material	Initial weight, (mg)	Heating rate, (K/min)	Temperature range, (K)	Onset temperature, T_o, (K)	End temperature T_e, (K)	Peak Temperature T_m, (K)
LDPE	6.29	5	303–873	691.6	754.7	735.2
	6.46	10	303–873	706.5	765.9	746.1
	6.56	15	303–873	718.8	774.2	754.2
	6.51	20	303–873	722.1	778.5	757.2
	6.06	30	303–873	727.2	786.6	765.1
	6.03	40	303–873	741.8	792.9	771.2
	6.02	50	303–873	739.8	799.6	778.2
HDPE	6.89	5	303–973	698.3	753.3	736.2
	6.94	10	303–973	699.6	766.4	748.4
	6.88	15	303–973	712.2	774.3	758.2
	6.67	20	303–973	723.8	779.1	763.4
	6.55	30	303–973	730.1	789.1	769.1
	7.09	40	303–973	741.3	795.8	773.4
	6.46	50	303–973	746.2	799.4	778.1
PP	8.03	5	303–973	670.6	724.6	705.5
	7.49	10	303–973	681.6	742.2	721.1
	7.34	15	303–973	687.1	753.5	732.2
	7.54	20	303–973	696.3	760.8	739.6
	7.33	30	303–973	707.2	771.1	749.7
	7.87	40	303–973	710.5	777.9	757.9
	7.29	50	303–973	712.1	783	762.4
PLA	6.65	5	303–973	573.3	625.6	613.1
	6.51	10	303–973	595.8	646.5	633.1
	6.26	15	303–973	604.7	654.6	642.1
	6.83	20	303–973	609.1	662.0	647.1
	6.57	30	303–973	612.5	665.1	651.2
	6.63	40	303–973	620.0	675.0	660.1
	6.73	50	303–973	632.3	687.4	669.1

indicate that higher heating rate delays the degradation rate, which leads to the shifting of onset, end and peak temperatures to higher values. This shift is mainly due to the time and temperature history subjected to the materials. From TGA curves it can be observed that the shape of the weight loss curve does not change with the variation of heating rate. Although, the obtained lone peak of DTG plot suggests that the overall degradation takes place in a single step (continuous degradation), but in real the thermal degradation of plastics proceeds as multistep scission reaction including parallel and series reactions. The lone peak actually combines all the reactions together (overlapped) and demonstrates the overall rate of degradation. Previous studies [19,34–36] also observed similar degradation profiles for similar materials. The reason for the displacement of T_o, T_e and T_m to the higher temperature is argued by many due to the change in mechanism cause by increasing the heating rate. Many viewed it as because of inefficient heat transfer from the furnace to sample causing difference in temperature between furnace and sample at higher heating rates. Since, the sample size and the amount used for TGA is small enough to overlook any heat and mass transfer gradients, the change in mechanism due to different heating rates is more supportive in regard of this argument.

3.2. Kinetic analysis

The activation energy obtained by the isoconversional methods with respect to conversion (α) has been shown in Fig. 3 and range of activation energy obtained for all five isoconversional method has been listed in Table 5. Due to various approximations and mathematical formulation, the results differ slightly from one another. Certainly in all the methods gradual change of E_α with the extent of conversion (α) was observed. However, differential isoconversional methods like Friedman showed the largest spread of activation energy and the distributed profile is also discontinuous compared to other method. Although, Friedman method does not consider any approximation like integral methods so it is expected to give more accurate results but to apply differential method to integral data (e.g. TGA) requires numerical differentiation. Numerical differentiation brings noise in the data and smoothing the same also brings inaccuracy, which ultimately leads to the discontinuous activation energy profile. The distributed activation energy (E_α) obtained from isoconversional method is the first of the

Table 5
Kinetic parameters (range) obtained using various isoconversional techniques.

Material	Isoconversional methods	E_α (kJ/mol)	A_α (min^{-1})	$f(\alpha)$[a]
LDPE	Friedman	178–256	2.79×10^{11}–1.64×10^{17}	R2
	OFW	165–242	5.77×10^{10}–1.78×10^{16}	
	KAS	162–242	3.67×10^{10}–1.72×10^{16}	
	Starink	148–222	4.07×10^{09}–8.44×10^{14}	
	AIC	170–231	9.19×10^{10}–3.59×10^{15}	
HDPE	Friedman	134–258	1.89×10^{08}–2.34×10^{17}	R2
	OFW	146–242	1.26×10^{09}–1.57×10^{16}	
	KAS	146–241	1.18×10^{09}–1.52×10^{16}	
	Starink	146–240	1.06×10^{09}–1.23×10^{16}	
	AIC	143–233	8.06×10^{08}–4.29×10^{15}	
PP	Friedman	124–187	4.74×10^{07}–4.98×10^{12}	R3
	OFW	140–176	5.77×10^{08}–9.65×10^{11}	
	KAS	136–173	3.22×10^{08}–5.91×10^{11}	
	Starink	136–173	2.92×10^{08}–5.16×10^{11}	
	AIC	133–173	1.82×10^{08}–5.48×10^{11}	
PLA	Friedman	97–120	1.28×10^{07}–3.25×10^{09}	R2
	OFW	113–129	1.92×10^{07}–1.58×10^{10}	
	KAS	99–113	1.80×10^{07}–1.01×10^{09}	
	Starink	108–124	8.62×10^{07}–6.95×10^{09}	
	AIC	99–116	1.60×10^{07}–1.41×10^{09}	

[a] The reaction model $f(\alpha)$ was predicted by Criados masterplot technique.

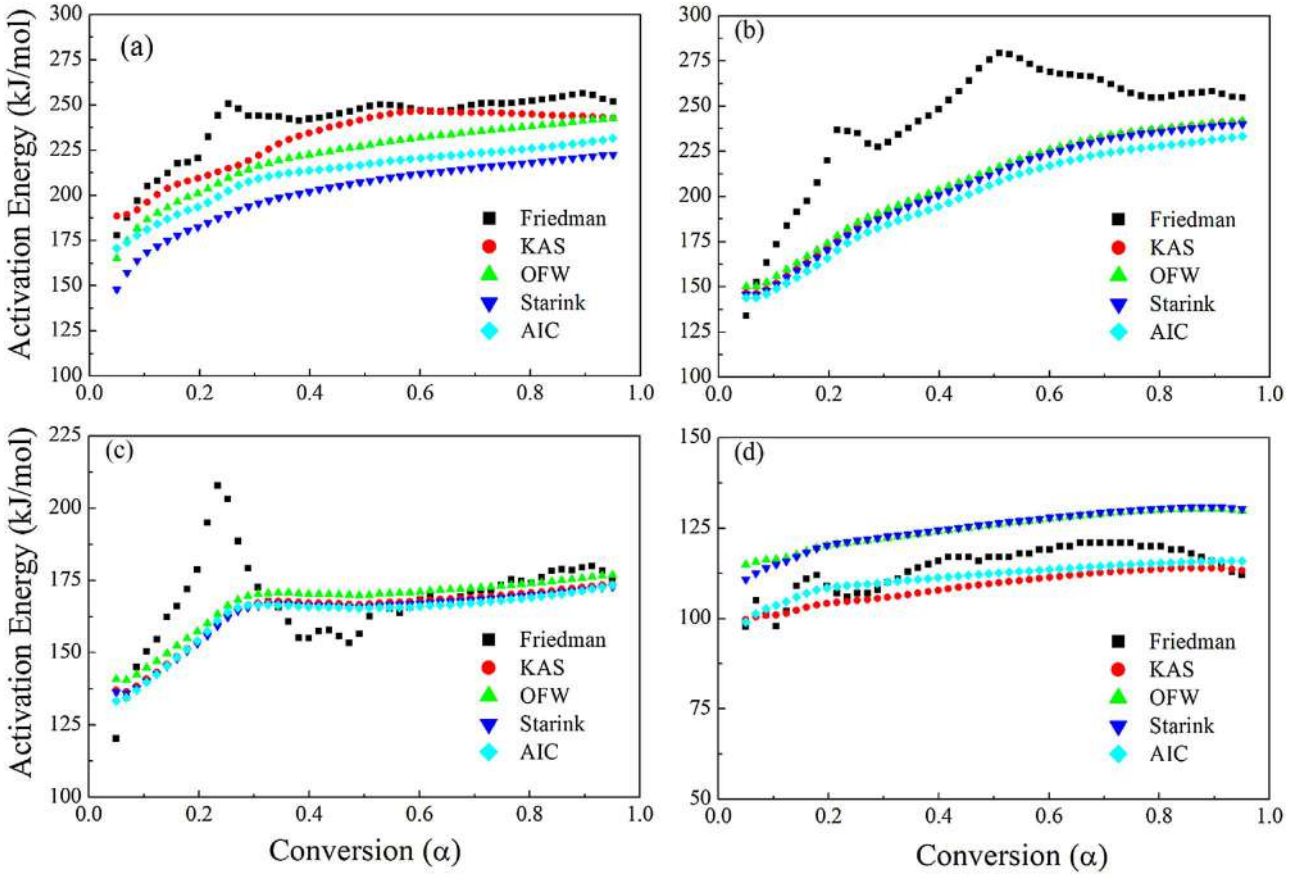

Fig. 3. Distribution of activation energy (E_α) from various isoconversional methods for (a) LDPE, (b) HDPE, (c) PP and (d) PLA.

three kinetic triplets, which is then substituted into linear logarithmic Arrhenius kinetic equation (Eq. (4)) to calculate $A\ f(\alpha)$ for each conversion point. Fig. 4 shows both activation energy distribution with associate uncertainties and $A\ f(\alpha)$ as a function of conversion for all four materials obtained from AIC method. The distribution of activation energy obtained from AIC method ranges 170–232 kJ/mol for LDPE, 143–231 kJ/mol for HDPE, 133–173 kJ/mol for PP and 99–116 kJ/mol for PLA. The values $A\ f(\alpha)$ further allow the calculation of variable pre-exponential factor (A_α), once the reaction model ($f(\alpha)$) is established with the help of masterplots.

The overall activation energy values of all four materials differ due to their molecular structures. During thermal treatment, the polyolefins; LDPE, HDPE and PP decompose into smaller hydrocarbons of various kinds [20]. Thermal stability of polyolefins strongly affected by branching. In PP every other carbon atom in the main polymer chain is a tertiary carbon, which provide more weak links for the starting of the degradation reaction. Degradation of both PE and PP occur via random scission followed by radical transfer process. An increase in effective activation energy with the progress of reaction for PE (LDPE and HDPE) and PP is caused by shift of the rate limiting step from initiation to the degradation initiated by the random scission. The degradation of plastics actually involves the breaking of the bonds between individual atoms forming the polymer chain. The breaking of C—C bond (~350 kJ/mol) requires higher activation energy and the degradation occurs above 400 °C temperature. But the degradation starts easily because of thermally labile bonds (weak links like branching and head to head links) inherent with the polymer chain. This explains the low activation energy at the beginning of the process [18].

On the other hand, PLA is a linear aliphatic hydrocarbon polymer which is produce from renewable resources and, degrades biologically. It has low activation energy compared to the polyolefins and the variation of activation energy is minimum. In thermal degradation process, PLA undergoes end chain scission involving OH group and random scission at the main polymer chain involving alkyl-oxygen homolysis or acyl-oxygen homolysis. Low activation energy of PLA degradation may speculate the low energy of non-radical backbiting ester interchange reactions involving OH chain ends [37,38]. Structure of PLA with the presence of alkyl or acyl-oxygen group makes it thermally less stable than polyolefins.

To calculate the values of pre-exponential factor (A_α) from $Af(\alpha)$, the reaction model $f(\alpha)$ was determined with the help of Criados masterplots [32]. All the models and associated functions, $f(\alpha)$ and $g(\alpha)$ used in Criado method are shown in Table 3. The theoretical masterplots $z(\alpha)/z(0.5)$ vs α for different mechanisms along with experimental reduced plots for all four materials are illustrated in Fig. 5(a) at a heating rate of 5 K/min. The ultimate selection of the reaction model was done on the basis of regression coefficient (R^2) between experimental and theoretical masterplots considering all heating rates (Fig. 5(b)). The degradation kinetic models for LDPE, HDPE, PP and PLA were found to be R2, R2, R3 and R2 respectively. Both R2 and R3 are geometrical contraction models, and assume that rate of degradation reaction starts at the surface and rate is controlled by the resulting interface reaction progress toward the centre. R2 and R3 differ in particle shape; R2 generally considered as contracting cylinder or contracting area and R3 represents contracting sphere or contracting volume [39]. Obtained models also resemble with the reaction models reported by Aboulkas et al. [36]and Guitiérrez and Palza [40]. Pre-exponential factor (A_α) values, at various extensions of conversion calculated with the help of identified model $f(\alpha)$ are shown in Fig. 6 and the range has been listed in Table 5. The linear relationship between the logarithmic form of preexponential factor and the activation energy is shown in Fig. 7. The linearity coefficient close to 1 ($R^2 \approx 1$) indicates that for all heating rates the values of A_α accord with the distributed activation energy for all the stages of degradation process. Comparable values of kinetic parameters achieved by previous studies using various methods in literature are listed in Table 6. The application of various kinetic methods, temperature programs and materials used in previous studies produced variations in kinetic values obtained, although most of the results are as per with the findings in the current study (Table 5).

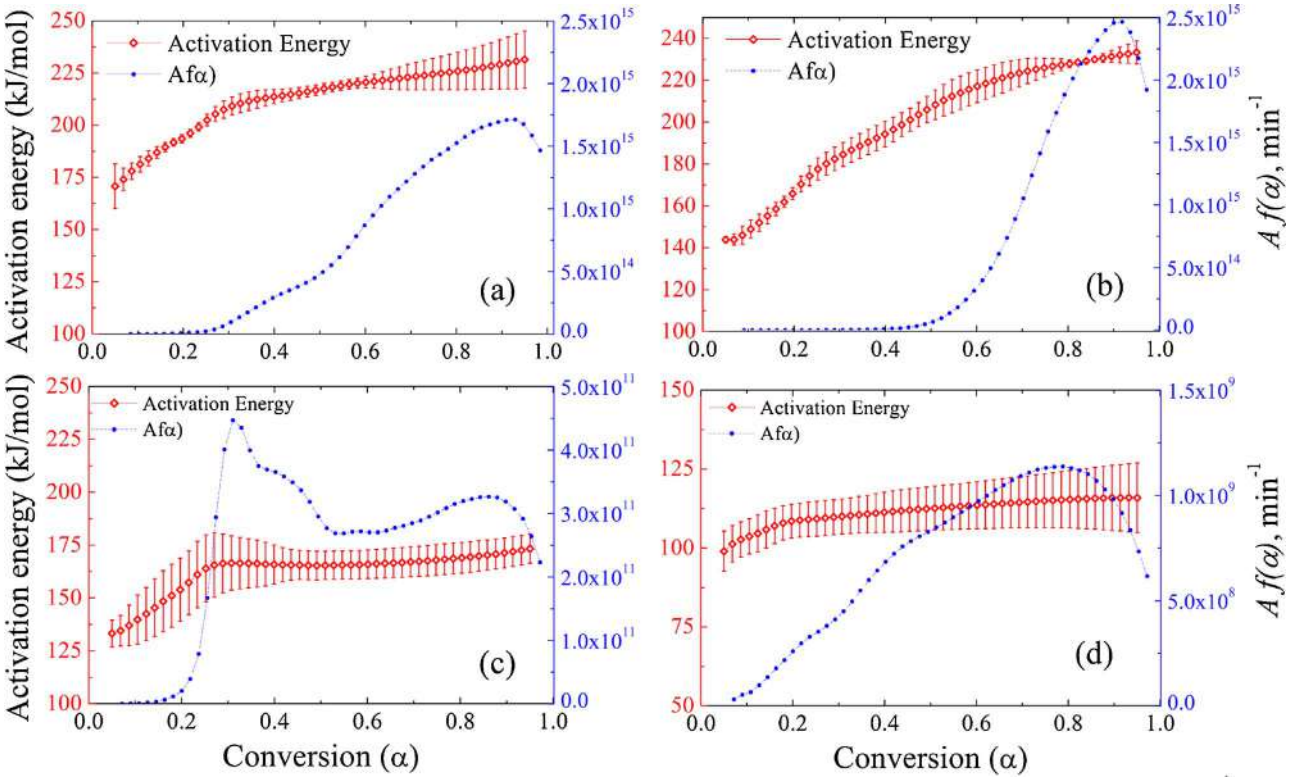

Fig. 4. Distribution of activation energy (E_α) (with uncertainty) and $(A \cdot f(\alpha))_\alpha$ values for (a) LDPE (b) HDPE (c) PP and (d) PLA.

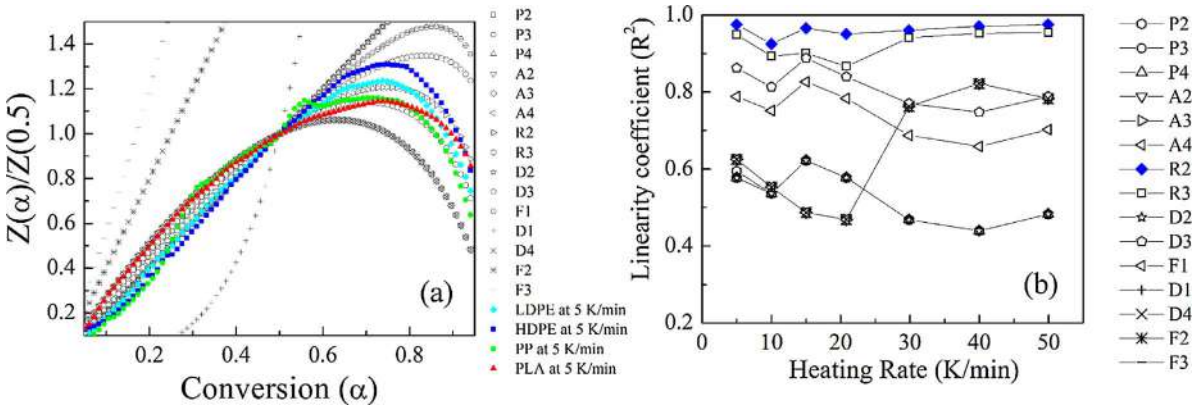

Fig. 5. (a) Theoretical masterplots of different reaction models and experimental reduced rate plot at 5 K/min for all four plastic samples and (b) Selection of the reaction model based on linearity coefficient ($R^2 \approx 1$) considering all seven heating rates (For LDPE) as an example.

3.3. Kinetic method selection

The choice of a particular model can be assured based on the deviation from the original path by evaluating statistical parameter like linearity regression coefficient R^2. The kinetic parameters (E_α and $A_\alpha f(\alpha)$) obtained from different models were subjected to reconstruct the conversion and temperature (α- T) profiles. MATLAB2015 software was used to solve the differential form of equation numerically considering temperature as independent variables with initial value taken from onset point of TGA curve. Similar methodology was used for constructing the α–T data for all the material at experimental heating rates and also at extrapolated heating rates. The comparison of simulated results (AIC method only) with experimental data for all four materials (Fig. 8) were found in good agreement. To ensure the similarity between experimental results with simulated profiles the regression analysis for all the heating rates was performed. The linearity was determined by calculating the regression coefficient (R^2) for each heating rate considered. Fig. 9 shows the comparison of average regression coefficients (R^2) for seven heating rates for all the methods considered in this study. A model selected for kinetic analysis should be able to reproduce the data and extrapolate the profile to the conditions, experiments not performed. Overall, the R^2 average analysis suggests that the AIC method is more appropriate to capture the complexity of the thermal degradation process of a material having better R^2 value. This may be due to the regress data sampling for small temperature interval adopted in the analysis for each heating rate considered. Due to the optimization by minimization of the function (Eq. (7)), AIC model is more accurate for a large pool of data collected at wide range and as well as more number of heating rates. To further validate the obtained kinetic parameters beyond the range of the temperature profiles used in kinetic analysis, two extrapolated degradation profiles at heating rate of 1 K/min and 100 K/min were simulated. The simulated kinetic profiles then compared with the experimental profiles obtained at the same heating rates for LDPE is shown in Fig. 10. The linear regression coefficient (R^2) between experimental and simulated profiles of LDPE were found to be 0.98 and 0.99 for the heating rates of 1 K/min and 100 K/

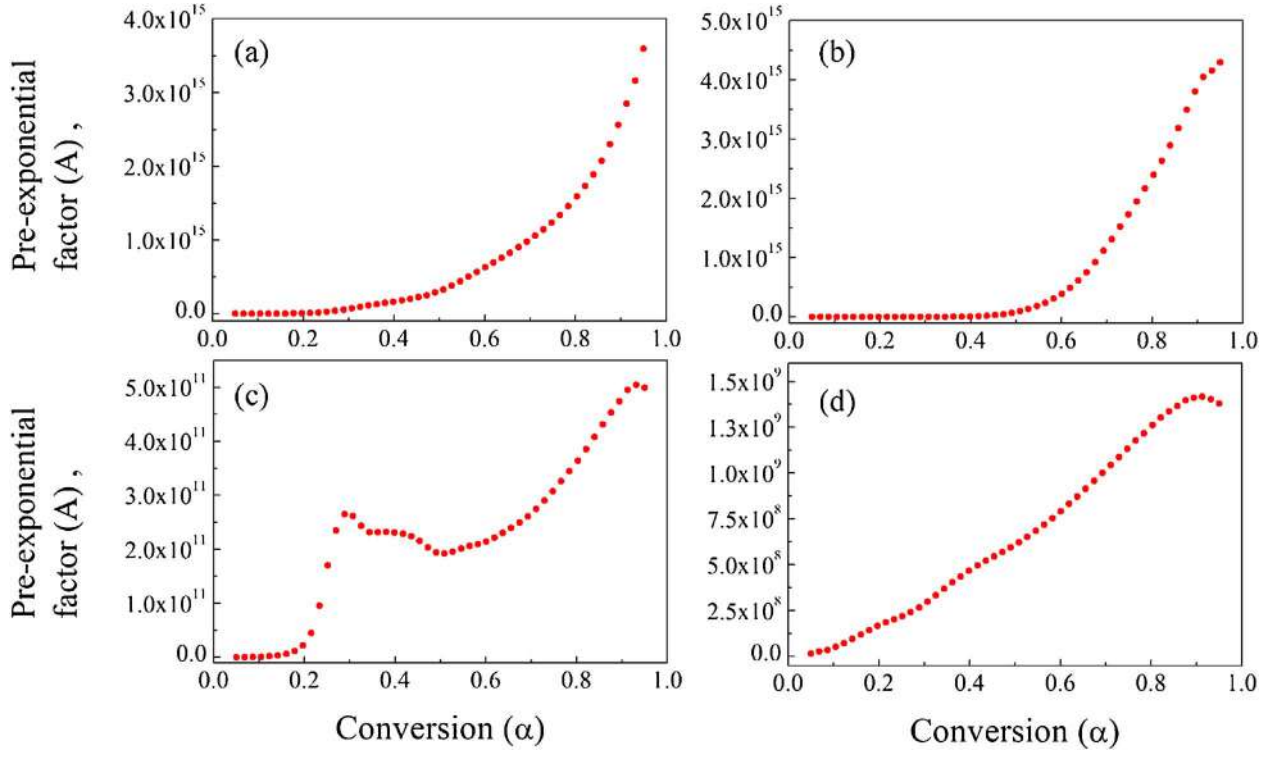

Fig. 6. Distributed pre-exponential (A_α) factor with the extension of conversion for (a) LDPE, (b) HDPE, (c) PP and (d) PLA obtained from AIC method by incorporating reaction models determined using Criados masterplots method.

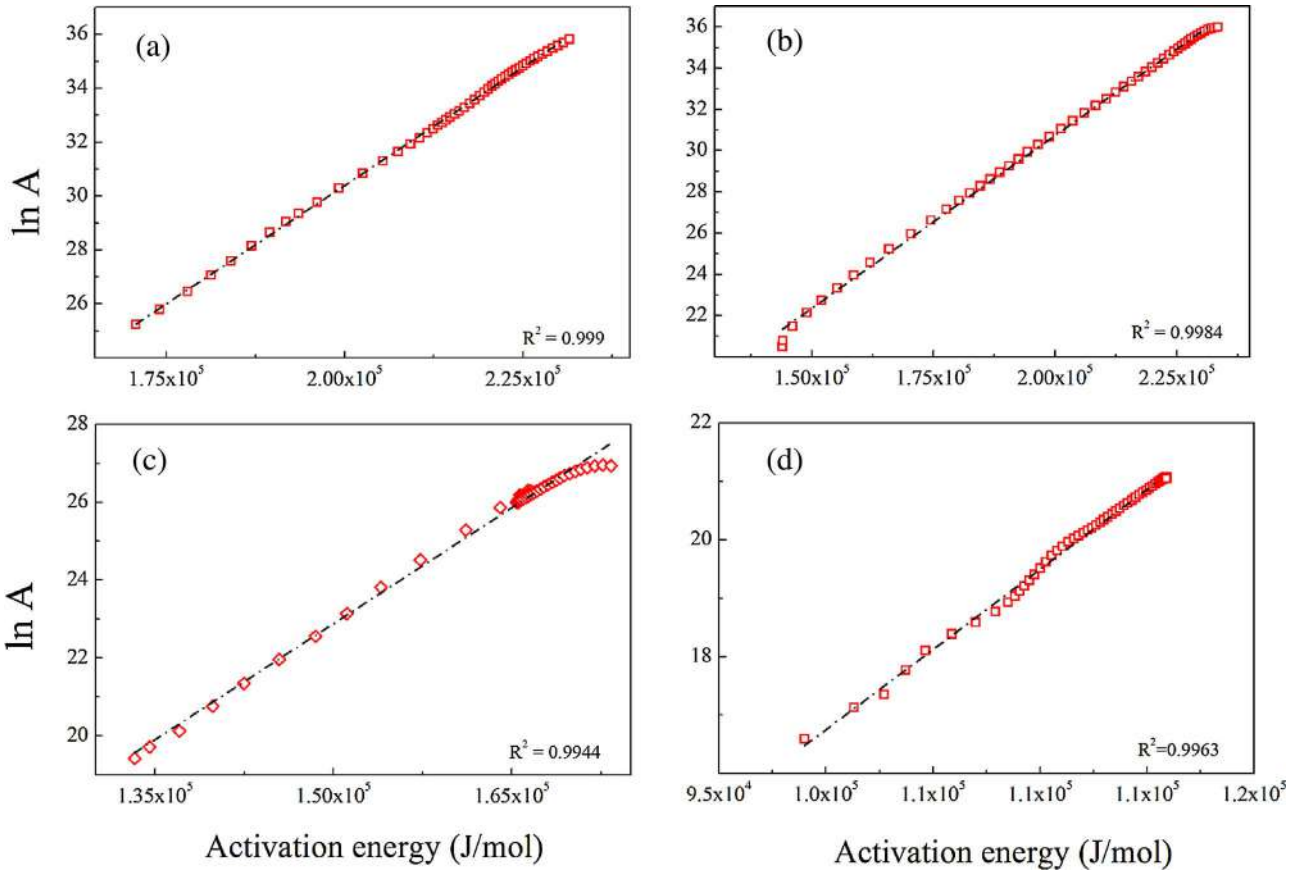

Fig. 7. Constable plot between logarithmic pre-exponential factor and activation energy calculated by AIC for (a) LDPE, (b) HDPE, (c) PP and (d) PLA.

Table 6
Kinetic parameters reported in literature using various methods.

Material	*E* (kJ/mol)	*A*(1/s)	*f(α)*	Method	References
LDPE	222	–	n^{th} order; n = 0.7	DTG curve fitting	[35]
	221 ± 3	–	R2	FR	[36]
	215 ± 8	–	R2	KAS	[36]
	218 ± 7	–	R2	OFW	[36]
	150–240	–	–	AIC	[20]
	100–220	–	–	Direct integration	[41]
	176–245	–	–	AIC	[35]
	178–190	–	–	AIC	[21]
HDPE	240	3.4×10^{16}	n^{th} order; n = 0.56	DTG curve fitting	[42]
	247 ± 5	–	R2	FR	[36]
	238 ± 11	–	R2	KAS	[36]
	243 ± 11	–	R2	OFW	[36]
PP	126	–	n^{th} order; n = 0.5	DTG curve fitting	[42]
	53–194	–	–	FR	[43]
	188 ± 6	–	R3	FR	[36]
	179 ± 8	–	R3	KAS	[36]
	183 ± 8	–	R3	OFW	[36]
	150–250	–	–	AIC	[20]
	106–134	–	–	AIC	[35]
	215 ± 9	–	–	FR	[40]
	203 ± 6	–	–	Starink	[40]
	204 ± 6	–	–	OFW	[40]
	203 ±	–	–	KAS	[40]
	52–145	9.58–4846	–	AIC	[20]
PLA	161–177.5	–	–	OFW	[44]
	172–183.6	–	–	FR	[44]
	174.7 ± 16.5	3.97×10^4–5.68×10^5	–	IKP method	[45]
	215	5.32×10^7	nth order; n = 0.5	Coats-Redfern	[46]
	170	–	–	OFW	[47]

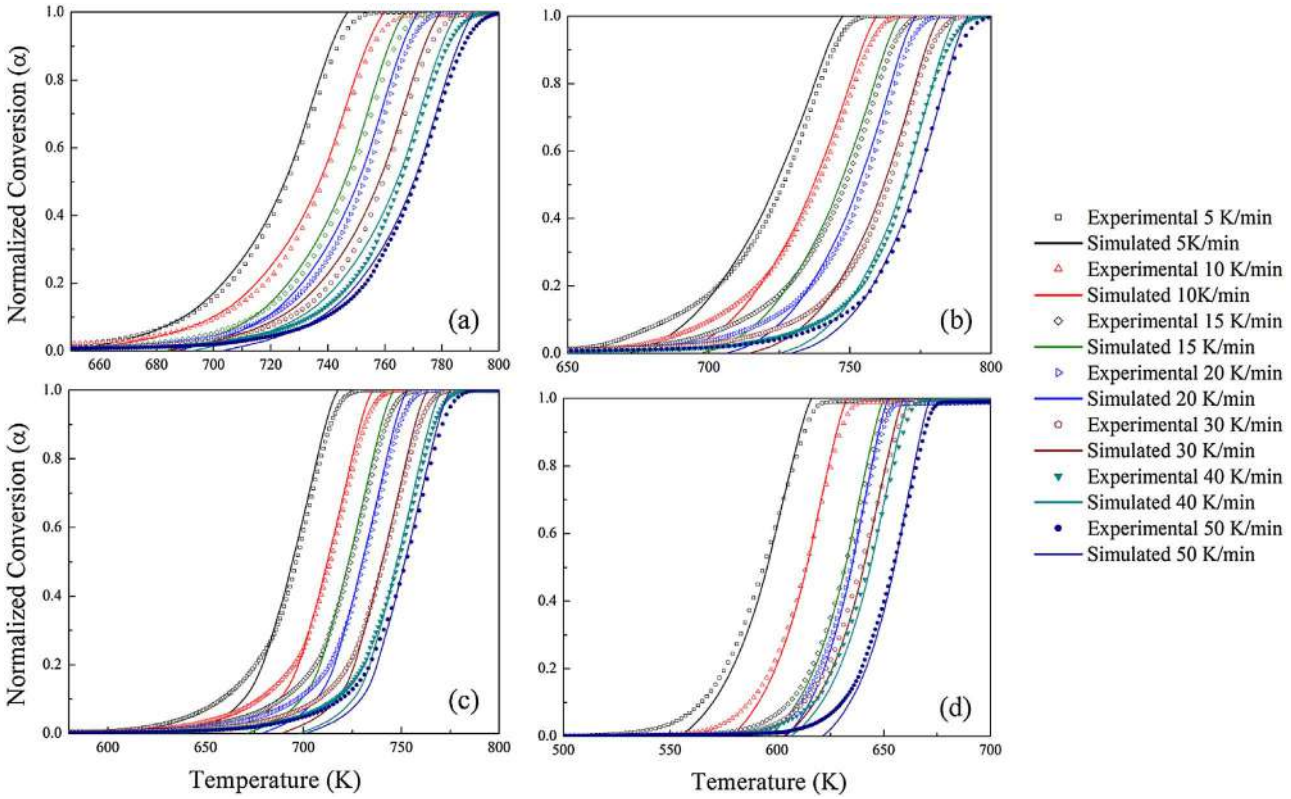

Fig. 8. Experimental and simulated (using AIC method) conversion profiles at various heating rates for (a) LDPE, (b) HDPE, (c) PP and (c) PLA.

min respectively. The degradation step (α-T) varies with varying heating rates lead to low onset & end degradation temperatures at lower heating rates (slow pyrolysis) whereas the degradation temperatures are shifted to higher temperatures at high heating rates (fast pyrolysis).

4. Conclusion

TGA based thermal degradation kinetics of four plastic materials were studied using isoconversional models. The kinetic study concludes that PLA needs less activation energy than PE and PP to degrade thermally. Within a variety of kinetic models available for thermal degradation, it is difficult to choose one model which can extract appropriate kinetic parameters from complex reaction mechanisms occurring. The continuous change in E values with α explains the change in mechanism of degradation and it was found to be important in the early and end stages of the degradation process. Isoconversional models

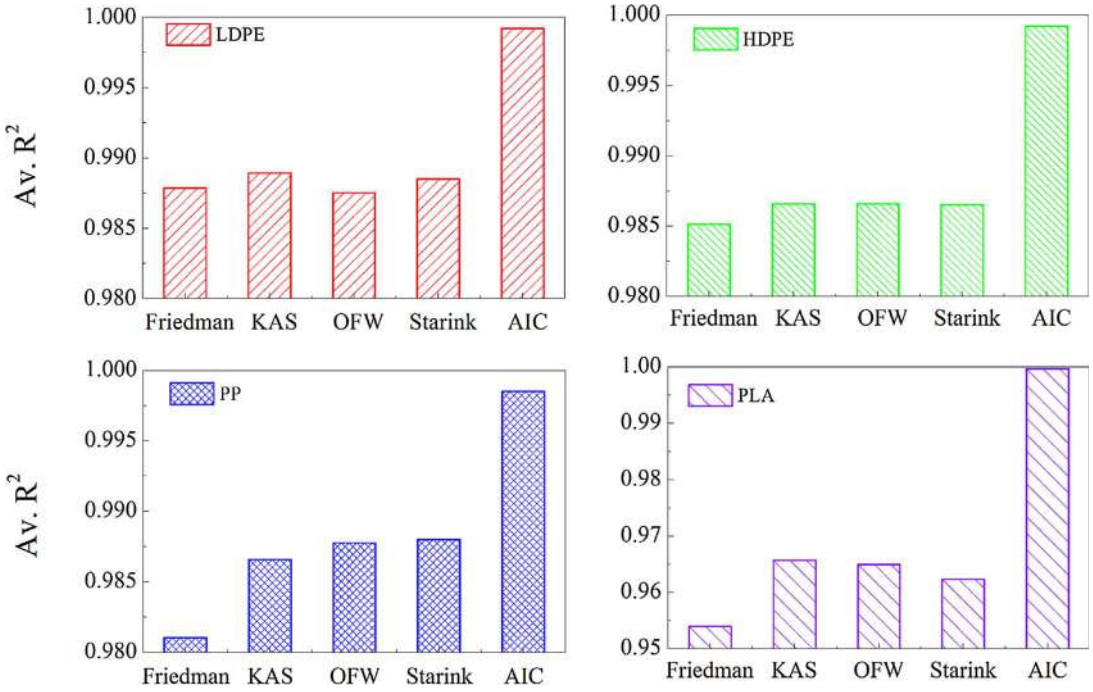

Fig. 9. Comparison of different isoconversional methods based on average linearity coefficient (R^2) between experimental reconstructed plots.

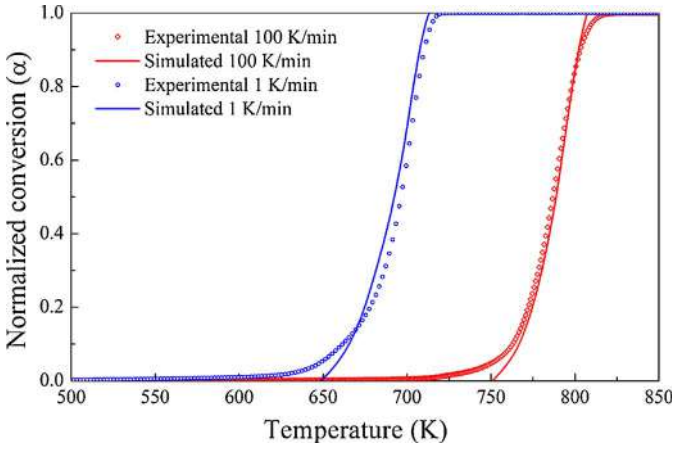

Fig. 10. Fitness of the extrapolated simulated profiles (α-T) at 1 K/min and 100 K/min for LDPE using the kinetic values obtained from AIC method.

are able to capture the reaction mechanism as kinetics follow the reaction progress. The advanced isoconversional method uses an optimization function to calculate the kinetic parameters and produces fewer errors (better R^2) for multiple heating rate data. Lower activation energy at the beginning of the degradation process refers that the initiation of degradation starts at weaker links of the polymer chain mostly follows side chain scission. In later stages the degradation follows random chain scission, where the polymer chain breaks at any random position and forming various monomers and oligomers. The exact mechanism can be determined by any model fitting method using different reaction models *f(α)* or *g(α)*. However, the kinetic analysis is also very subjective to the reaction configuration and data sampling, careful analysis of onset points.

Acknowledgements

Authors would like to acknowledge the financial support (Grant# YSS/2014/000837) provided by Department of Science and Technology (DST), Government of India. Authors also acknowledge the centre of excellence for sustainable polymer (CoE-Suspol) at Indian Institute of Technology Guwahati, India for providing the samples.

References

[1] CPCB, TERI Energy Data Directory and Yearbook, TERI Press, 2010, pp. 333–334.
[2] A. Demirbas, Pyrolysis of municipal plastic wastes for recovery of gasoline-range hydrocarbons, J. Anal. Appl. Pyrolysis 72 (2004) 97–102.
[3] M. Erceg, T. Kovačić, I. Klarić, Dynamic thermogravimetric degradation of poly(3-hydroxybutyrate)/aliphatic–aromatic copolyester blends, Polym. Degrad. Stab. 90 (2005) 86–94.
[4] V.B. Carmona, A. de Campos, J. Marconcini, L.H.C. Mattoso, Kinetics of thermal degradation applied to biocomposites with TPS, PCL and sisal fibers by non-isothermal procedures, J. Therm. Anal. Calorim. 115 (2013) 153–160.
[5] J.W. Bujak, Thermal utilization (treatment) of plastic waste, Energy 90 (2015) 1468–1477.
[6] M.E. Brown, M. Maciejewski, S. Vyazovkin, R. Nomen, J. Sempere, A.K. Burnham, J. Opfermann, R. Strey, H.L. Anderson, A. Kemmler, R. Keuleers, J. Janssens, H.O. Desseyn, C. Li, T.B. Tang, B. Roduit, J. Malek, T. Mitsuhashi, Computational aspects of kinetic analysis Part A: The ICTAC kinetics project-data, methods and results, Thermochim. Acta 355 (2000) 125–143.
[7] A.K. Burnham, Computational aspects of kinetic analysis. Part D: The ICTAC kinetics project-multi-thermal-history model-fitting methods and their relation to isoconversional methods, Thermochim. Acta 355 (2000) 165–170.
[8] M. Maciejewski, Computational aspects of kinetic analysis. Part B: The ICTAC Kinetics Project – the decomposition kinetics of calcium carbonate revisited or some tips on survival in the kinetic minefield, Thermochim. Acta 355 (2000) 145–154.
[9] S. Vyazovkin, Computational aspects of kinetic analysis. Part C. The ICTAC Kinetics Project – the light at the end of the tunnel? Thermochim. Acta 355 (2000) 155–163.
[10] S. Vyazovkin, A.K. Burnham, J.M. Criado, L.A. Pérez-Maqueda, C. Popescud, N. Sbirrazzuolie, ICTAC Kinetics Committee recommendations for performing kinetic computations on thermal analysis data, Thermochim. Acta 520 (2011) 1–19.
[11] S. Vyazovkin, K. Chrissafis, M.L. Di Lorenzo, N. Koga, M. Pijolat, B. Roduit, N. Sbirrazzuoli, J.J. Suñol, ICTAC Kinetics Committee recommendations for collecting experimental thermal analysis data for kinetic computations, Thermochim. Acta 590 (2014) 1–23.
[12] S. Vyazovkin, C.A. Wight, Isothermal and non-isothermal kinetics of thermally stimulated reactions of solids, Int. Rev. Phys. Chem. 17 (1998) 407–433.
[13] H.L. Friedman, Kinetics of thermal degradation of char-forming plastic from thermogravimetry. application to a phenolic plastic, J. Polym. Sci. Part C 6 (1964) 183–195.
[14] J.H. Flynn, L.A. Wall, General treatment of thermogravinetry of polymers, J. Res. Natl. Bur. Stand.-A Phys. Chem. 70A (1966) 487–523.
[15] J.H. Flynn, The isoconversional method for determination of energy of activation at constant heating rates, J. Therm. Anal. 27 (1983) 95–102.
[16] T.S. Akahira, T. Sunose, Method of Determining Activation Deterioration Constant of Electrical Insulating Materials Research Report vol. 16, China Institute of Technology (Science Technology), 1971, pp. 22–31.
[17] M.J. Starink, The determination of activation energy from linear heating rate experiments: a comparison of the accuracy of isoconversion methods, Thermochim. Acta 404 (2003) 163–176.
[18] S. Vyazovkin, N. Sbirrazzuoli, Isoconversional kinetic analysis of thermally stimulated processes in polymers, Macromol. Rapid Commun. 27 (2006) 1515–1532.
[19] S. Khedri, S. Elyasi, Kinetic analysis for thermal cracking of HDPE: a new isoconversional approach, Polym. Degrad. Stab. 129 (2016) 306–318.
[20] J.D. Peterson, S. Vyazovkin, C.A. Wight, Kinetics of the thermal and thermo-oxidative degradation of polystyrene, polyethylene and poly(propylene), Macromol. Chem. Phys. 202 (2001) 775–784.
[21] B. Saha, A.K. Ghoshal, Model-free kinetics analysis of decomposition of polypropylene over Al-MCM-41, Thermochim. Acta 460 (2007) 77–84.
[22] C. He, Y. Wang, Y. Luo, L. Kong, Z. Peng, Thermal degradation kinetics and mechanism of epoxidized natural rubber, J. Polym. Eng. 33 (2013) 331–335.
[23] G. Mishra, T. Bhaskar, Non isothermal model free kinetics for pyrolysis of rice straw, Bioresour. Technol. 169 (2014) 614–621.
[24] L.N. Samuelsson, M.U. Babler, R. Moriana, A single model-free rate expression describing both non-isothermal and isothermal pyrolysis of Norway Spruce, Fuel 161 (2015) 59–67.
[25] A.A. Jain, A. Mehraa, V.V. Ranade, Processing of TGA data: analysis of isoconversional and model fitting methods, Fuel 165 (2016) 490–498.
[26] L.N. Samuelsson, R. Moriana, M.U. Babler, M. Ek, K. Engvall, Model-free rate expression for thermal decomposition processes: the case of microcrystalline cellulose pyrolysis, Fuel 143 (2015) 438–447.
[27] A. Zotti, A. Borriello, M. Ricciardi, V. Antonucci, M. Giordano, M. Zarrelli, Effects of sepiolite clay on degradation and fire behaviour of a bisphenol A-based epoxy, Compos. Part B-Eng. 73 (2015) 139–148.
[28] P. Rajeshwari, T.K. Dey, Advanced isoconversional and master plot analyses on non-isothermal degradation kinetics of AlN (nano)-reinforced HDPE composites, J. Therm. Anal. Calorim. 125 (2016) 369–386.
[29] J.R. Opfermann, E. Kaisersberger, H.J. Flammersheim, Model-free analysis of thermoanalytical data-advantages and limitations, Thermochim. Acta 391 (2002) 119–127.
[30] P. Tiwari, M. Deo, Detailed kinetic analysis of oil shale pyrolysis TGA data, AIChE J. 58 (2012) 505–515.
[31] S. Vyazovkin, C.A. Wight, Kinetics in solids, Ann. Rev. Phys. Chem. 48 (1997) 125–149.
[32] J.M. Criado, Kinetic analysis of DTG data from master curve, Thermochim. Acta 24 (1978) 186–189.
[33] F.H. Constable, The mechanism of catalytic decomposition, Proc. R. Soc. Lond. 108 (1923) 355–378.
[34] C.H. Wu, C.Y. Chang, J.L. Hor, S.M. Shin, L.W. Chen, F.W. Chang, On the thermal treatment of plastic mixtures of MSW: Pyrolysis kinetics, Waste Manag. 13 (1993) 221–235.
[35] A.C.K. Chowlu, P.K. Reddy, A.K. Ghoshal, Pyrolytic decomposition and model-free kinetics analysis of mixture of polypropylene (PP) and low-density polyethylene (LDPE), Thermochim. Acta 485 (2009) 20–25.
[36] A. Aboulkas, K. El harfi, A. El Bouadili, Thermal degradation behaviors of polyethylene and polypropylene. Part I: pyrolysis kinetics and mechanisms, Energy Convers. Manag. 51 (2010) 1363–1369.
[37] I.C. McNeill, H.A. Leiper, Degradation studies of some polyesters and polycarbonates-2. Polylactide: degradation under isothermal conditions, thermal degradation mechanism and photolysis of the polymer, Polym. Degrad. Stab. 11 (1985) 309–326.
[38] I.C. McNeill, H.A. Leiper, Degradation studies of some polyesters and polycarbonates-1. Polylactide: general features of the degradation under programmed heating condition, Polym. Degrad. Stab. 11 (1985) 267–285.
[39] A. Khawam, D.R. Flanagan, Solid-state kinetic models: basics and mathematical fundamentals, J. Phys. Chem. B 110 (2006) 17315–17328.
[40] O. Gutiérrez, H. Palza, Effect of carbon nanotubes on thermal pyrolysis of high density polyethylene and polypropylene, Polym. Degrad. Stab. 120 (2015) 122–134.
[41] B. Saha, A.K. Ghoshal, Model-free kinetics analysis of waste PE sample, Thermochim. Acta 451 (2006) 27–33.
[42] J. Yang, R. Miranda, C. Roy, Using the DTG curve fitting method to determine the apparent kinetic parameters of thermal decomposition of polymers, Polym. Degrad. Stab. 73 (2001) 455–461.
[43] J.H. Chan, S.T. Balke, The thermal degradation kinetic of kinetics of polypropylene: part III. Thermogravemetric analysis, Polym. Degrad. Stab. 57 (1997) 135–149.
[44] H. Zou, C. Yi, L. Wang, H. Liu, W. Xu, Thermal degradation of poly(lactic acid)

measured by thermogravimetry coupled to Fourier transform infrared spectroscopy, J. Therm. Anal. Calorim. 97 (2009) 929–935.
[45] J. Li, W. Zheng, L. Li, Y. Zheng, X. Lou, Thermal degradation kinetics of g-HA/PLA composite, Thermochim. Acta 493 (2009) 90–95.
[46] W. Gang, L. Aimin, Thermal decomposition and kinetics of mixtures of polylactic acid and biomass during copyrolysis, Chin. J. Chem. Eng. 16 (2008) 929–933.
[47] R. Valapa, G. Pugazhenthi, V. Katiyar, Thermal degradation kinetics of sucrose palmitate reinforced poly(lactic acid) biocomposites, Int. J. Biol. Macromol. 65 (2014) 275–283.